

1 **A *k*-mer-based method for the identification of phenotype-associated**
2 **genomic biomarkers and predicting phenotypes of sequenced bacteria.**

3

4 Erki Aun¹, Age Brauer¹, Veljo Kisand², Tanel Tenson², Mairo Remm¹

5

6 ¹Department of Bioinformatics, Institute of Molecular and Cell Biology, University of Tartu, Estonia

7 ²Institute of Technology, University of Tartu, Estonia

8

9 *Corresponding author:

10 E-mail: erki.aun@ut.ee

11

12 **Abstract**

13 We have developed an easy-to-use and memory-efficient method called PhenotypeSeeker that (a)
14 generates a k -mer-based statistical model for predicting a given phenotype and (b) predicts the
15 phenotype from the sequencing data of a given bacterial isolate. The method was validated on 167
16 *Klebsiella pneumoniae* isolates (virulence), 200 *Pseudomonas aeruginosa* isolates (ciprofloxacin
17 resistance) and 460 *Clostridium difficile* isolates (azithromycin resistance). The phenotype prediction
18 models trained from these datasets performed with 88% accuracy on the *K. pneumoniae* test set, 88%
19 on the *P. aeruginosa* test set and 96.5% on the *C. difficile* test set. Prediction accuracy was the same
20 for assembled sequences and raw sequencing data; however, building the model from assembled
21 genomes is significantly faster. On these datasets, the model building on a mid-range Linux server
22 takes approximately 3 to 5 hours per phenotype if assembled genomes are used and 10 hours per
23 phenotype if raw sequencing data are used. The phenotype prediction from assembled genomes takes
24 less than one second per isolate. Thus, PhenotypeSeeker should be well-suited for predicting
25 phenotypes from large sequencing datasets.

26 PhenotypeSeeker is implemented in Python programming language, is open-source software and is
27 available at GitHub (<https://github.com/bioinfo-ut/PhenotypeSeeker/>).

28 **Summary**

29 Predicting phenotypic properties of bacterial isolates from their genomic sequences has numerous
30 potential applications. A good example would be prediction of antimicrobial resistance and virulence
31 phenotypes for use in medical diagnostics. We have developed a method that is able to predict
32 phenotypes of interest from the genomic sequence of the isolate within seconds. The method uses
33 statistical model that can be trained automatically on isolates with known phenotype. The method is
34 implemented in Python programming language and can be run on low-end Linux server and/or on
35 laptop computers.

36

37 **Introduction**

38 The falling cost of sequencing has made genome sequencing affordable to a large number of labs, and
39 therefore, there has been a dramatic increase in the number of genome sequences available for
40 comparison in the public domain [1]. These developments have facilitated the genomic analysis of
41 bacterial isolates. An increasing amount of bacterial whole genome sequencing (WGS) data has led to
42 more and more genome-wide studies of DNA variation related to different phenotypes [2–7]. Among
43 these studies, antibiotic resistance phenotypes are the most concerning and have garnered high public
44 interest, especially since several multidrug-resistant strains have emerged worldwide [8]. The
45 detection of known resistance-causing mutations as well as the search for new candidate biomarkers
46 leading to resistance phenotypes requires reasonably rapid and easily applicable tools for processing
47 and comparing the sequencing data of hundreds of isolated strains. However, there is still a lack of
48 user-friendly software tools for the identification of genomic biomarkers from large sequencing
49 datasets of bacterial isolates [9,10].

50 Methods that are based on sequence alignment are limited because they are strongly dependent on the
51 availability of the list of previously described and confirmed resistance genes and mutations. New
52 variations relevant to a bacterial phenotype would be missed if we rely on known markers. In
53 addition, many bacterial species have extensive intra-species variation from small sequence-based
54 differences to the absence or presence of whole genes or gene clusters. Choosing only one genome as
55 a reference for searching for the variable components would be highly limiting.

56 *K*-mers, which are short DNA oligomers with length *k*, enable us to simultaneously discover a large
57 set of single nucleotide variations, insertions and deletions associated with the phenotypes under
58 study. The advantage of using *k*-mer-based methods in genomic biomarker discovery is that they do
59 not require sequence alignments and can even be applied to raw sequencing data. Several *k*-mer-based
60 tools for detecting the biomarkers behind different bacterial phenotypes have been previously
61 published. The SEER program takes either a discrete or continuous phenotype as an input, counts
62 variable-length *k*-mers and corrects for the clonal population structure [11]. SEER is a complex
63 pipeline requiring several separate steps for the user to execute and currently has many system-level

64 dependencies for successful compilation and installation. Another similar tool, Kover, handles only
65 discrete phenotypes, counts user-defined size k -mers and does not use any correction for population
66 structure [12]. The Neptune software targets so-called 'signatures' differentiating two groups of
67 sequences but cannot locate smaller mutations, such as single isolated nucleotide variations. The
68 'signatures' that Neptune detects are relatively large genomic loci, which may include genomic
69 islands, phage regions or operons [13].

70 We created PhenotypeSeeker as we observed the need for a tool that could combine all the benefits of
71 the programs available but at the same time would be easily executable and would take a reasonable
72 amount of computing resources without the need for dedicated high-performance computer hardware.

73

74 **Results**

75 **Implementation**

76 PhenotypeSeeker consist of two subprograms: 'PhenotypeSeeker modeling' and 'PhenotypeSeeker
77 prediction'. 'PhenotypeSeeker modeling' takes either assembled contigs or raw-read data as an input
78 and builds a statistical model for phenotype prediction. The method starts with counting all possible k -
79 mers from the input genomes, using the GenomeTester4 software package [14], followed by k -mer
80 filtering by their frequency in strains. Subsequently, the k -mer selection for regression analysis is
81 performed. In this step, to test the k -mers' association with the phenotype, the method applies Welch's
82 two-sample t-test if the phenotype is continuous and a chi-squared test if it is binary. Finally, the
83 logistic regression or linear regression model is built. The PhenotypeSeeker output gives the
84 regression model in a binary format and three text files, which include the following: (1) the results of
85 association tests, (2) the coefficients of k -mers in the regression model, (3) a FASTA file with
86 phenotype-specific k -mers, assembled to longer contigs when possible, and (4) a summary of the
87 regression analysis performed (Fig 1). Optionally, it is possible to use weighting for the strains to take
88 into account the clonal population structure. The weights are based on a distance matrix of strains
89 made with an alignment-free k -mer-based method called Mash [15]. The weights of each genome are
90 calculated using the Gerstein , Sonnhammer and Cothia method [16]. 'PhenotypeSeeker prediction'
91 uses the regression model generated by 'PhenotypeSeeker modeling' to conduct fast phenotype
92 predictions on input samples (Fig 1). Using gmer_counter from the FastGT package [17], the tool
93 searches the samples only for the k -mers used as parameters in the regression model. Predictions are
94 then made based on the presence or absence of these k -mers.

95 PhenotypeSeeker uses fixed-length k -mers in all analyses. Thus, the k -mer length is an important
96 factor influencing the overall software performance. The effects of k -mer length on speed, memory
97 usage and accuracy were tested on a *P. aeruginosa* ciprofloxacin dataset. A general observation from
98 that analysis is that the CPU time and the PhenotypeSeeker memory usage increase when the k -mer
99 length increases (Fig 2). Previously described mutations in the *P. aeruginosa* *parC* and *gyrA* genes
100 were always detected if the k -mer length was at least 13 nucleotides. We assume that in most cases, a

101 *k*-mer length of 13 is sufficient to detect biologically relevant mutations, although in certain cases,
102 longer *k*-mers might provide additional sensitivity. The *k*-mer length in PhenotypeSeeker is a user-
103 selectable parameter. Although most of the phenotype detection can be performed with the default *k*-
104 mer value, we suggest experimenting with longer *k*-mers in the model building phase. All subsequent
105 analyses in this article are performed with a *k*-mer length of 13, unless specified otherwise.

106 **Ciprofloxacin resistance phenotype in *Pseudomonas aeruginosa***

107 PhenotypeSeeker was applied to the datasets composed of *P. aeruginosa* genomes and corresponding
108 ciprofloxacin MIC-s. We built two separate models using a continuous phenotype for one and binary
109 phenotype for another. Binary phenotype values were created based on EUCAST ciprofloxacin
110 breakpoints [18]. Both models detected *k*-mers associated with mutations in quinolone resistance
111 determining regions (QRDR) of the *parC* (c.260C>T, p.Ser87Leu) and *gyrA* (c.248C>T, p.Thr83Ile)
112 genes (Fig 3, S2 File). These genes encode DNA topoisomerase IV subunit A and DNA gyrase
113 subunit A, the target proteins of ciprofloxacin [19]. Mutations in the QRDR regions of these genes are
114 well-known causes of decreased sensitivity to quinolone antibiotics, such as ciprofloxacin [20]. The
115 model built using a binary phenotype had a prediction accuracy of 88%, sensitivity of 90% and
116 specificity of 87% on the test subset. The coefficient of determination (R^2) of the test subset for the
117 continuous phenotype was 0.413 (S2 File).

118 **Azithromycin resistance phenotype in *Clostridium difficile***

119 In addition to the *P. aeruginosa* dataset, we tested a *C. difficile* azithromycin resistance dataset (S2
120 File) studied using Kover in Drouin et al., 2016 [12]. *ermB* and Tn6110 transposon were the
121 sequences known and predicted to be important in an azithromycin resistance model by Kover [12].
122 *ermB* was not located on the transposon Tn6110. PhenotypeSeeker found *k*-mers for both sequences
123 while using *k*-mers of length 13 or 16. Tn6110 is a transposon that is over 58 kbp long and contains
124 several protein coding sequences, including 23S rRNA methyltransferase, which is associated with
125 macrolide resistance [21]. The predictive models with all tested *k*-mer lengths (13, 16 and 18)
126 contained *k*-mers covering the entire Tn6110 transposon sequence, both in protein coding and non-
127 coding regions. In addition to the 23S rRNA methyltransferase gene, *k*-mers in all three models were

128 mapped to the recombinase family protein, sensor histidine kinase, ABC transporter permease, TlpA
129 family protein disulfide reductase, endonuclease, helicase and conjugal transfer protein coding
130 regions. The model built for the *C. difficile* azithromycin resistance phenotype had a prediction
131 accuracy of 96.5%, sensitivity of 96% and specificity of 97% on the test subset.

132 **Virulence phenotype in *Klebsiella pneumoniae***

133 In addition to antibiotic resistance phenotypes in *P. aeruginosa* and *C. difficile*, we used *K.*
134 *pneumoniae* human infection-causing strains as a different kind of phenotype example. *K.*
135 *pneumoniae* strains contain several genetic loci that are related to virulence. These loci include
136 aerobactin, yersiniabactin, colibactin, salmochelin and microcin siderophore system gene clusters
137 [22–26], the allantoinase gene cluster [27], *rmpA* and *rmpA2* regulators [28,29], the ferric uptake
138 operon *kfuABC* [30] and the two-component regulator *kvgAS* [31]. The model predicted by
139 PhenotypeSeeker for invasive/infectious phenotypes included 13-mers representing several of these
140 genes. Genes in colibactin (*clbQ* and *clbO*), aerobactin (*iucB* and *iucC*) and yersiniabactin (*irp1*, *irp2*,
141 *fyuA*, *ybtQ*, *ybtX*, and *ybtP*) clusters showed the most differentiating pattern between carrier and
142 invasive/infectious strains (Fig 4; S2 File). A 13-mer mapping to a gene-coding capsule assembly
143 protein Wzi was also represented in the model. The model built for *K. pneumoniae* invasive/infectious
144 phenotypes had a prediction accuracy of 88%, sensitivity of 91% and specificity of 78% on the test
145 subset.

146 **Classification accuracy and running time**

147 To measure the average classification accuracies of logistic regression models, all three datasets were
148 divided into a training and test set of approximately 75% and 25% of strains respectively. A *K*-mer
149 length of 13 was used, and a weighted approach was tested on binary phenotypes (Table 1). When
150 using sequencing reads instead of assembled contigs as the input, we required a minimum frequency
151 of 5 for a 13-mer to reduce the influence of sequencing errors. The PhenotypeSeeker prediction
152 accuracy is not lower when using raw sequencing reads instead of assembled genomes, and therefore,
153 assembly building is not required before model building. Our results with *K. pneumoniae* show that

154 PhenotypeSeeker can be successfully applied to other kinds of phenotypes in addition to antibiotic
155 resistance.

156 **Table 1. Model prediction accuracy and running time.** The results with 13-mers and weighting are
157 shown. The maximum number of 13-mers selected for the regression model was 1000. In cases where
158 sequencing reads were used as the input, a minimum frequency of 5 for a 13-mer was required to
159 reduce the influence of sequencing errors.

Dataset	Accuracy	Number of isolates		Time for the model building (per model)	Time for the phenotype prediction (per phenotype)
		Training	Testing		
<i>Pseudomonas aeruginosa</i> (contigs)	88.0%	150	50	3h 36m	0.81s
<i>Pseudomonas aeruginosa</i> (reads)	88.0%	150	50	19h 56m	58.0s
<i>Klebsiella pneumoniae</i> (contigs)	88.0%	125	42	3h 38m	0.74s
<i>Klebsiella pneumoniae</i> (reads)	88.0%	125	42	10h 3m	28.0s
<i>Clostridium difficile</i> (contigs)	96.5%	345	115	4h 50m	0.61s
<i>Pseudomonas aeruginosa</i> (contigs)	88.0%	150	50	3h 36m	0.81s

160

161 In our trials, the model building on a given dataset took 3 to 5 hours per phenotype, and prediction of
162 the phenotype took less than a second on assembled genomes (Table 1). The CPU time of model
163 building by PhenotypeSeeker depends mainly on the number of different *k*-mers in genomes of the
164 training set. The analysis performed on our 200 *P. aeruginosa* genomes showed that the CPU time of
165 the model building grows linearly with the number of genomes given as input (S1 Fig).

166 The memory requirement of PhenotypeSeeker did not exceed 2 GB if default parameter settings are
167 used, allowing us to run analyses on laptop computers (S2 Fig) if necessary. The p-value cut-offs
168 during the *k*-mer filtering step influence the number of *k*-mers included in the model and have a

169 potentially strong impact on model performance. The tables in the S1 File show the effects of
170 different p-value cut-offs on model performances.

171 **Comparison with other software**

172 We ran SEER and Kover on the same *P. aeruginosa* ciprofloxacin dataset and *C. difficile*
173 azithromycin resistance dataset to compare the efficiency and CPU time usage with PhenotypeSeeker.
174 In the *P. aeruginosa* dataset, SEER was able to detect *gyrA* and *parC* mutations only when resistance
175 was defined as a binary phenotype. In cases with a continuous phenotype, those *k*-mers did not pass
176 the p-value filtering step. Since Kover's aim is to create a resistance predicting model, not an
177 exhaustive list of significant *k*-mers, it was expected that not all the mutations would be described in
178 the output. *gyrA* variation already sufficiently characterized the resistant strains set, and therefore,
179 *parC* mutations were not included in the model. The same applies to the PhenotypeSeeker results with
180 16- and 18-mers. *parC*-specific 16- or 18-mers were included among the 1000 *k*-mers in the
181 prediction model (based on statistically significant p-values) but with the regression coefficient equal
182 to zero because they were present in the same strains as *gyrA* specific predictive *k*-mers.

183 In the *C. difficile* dataset, our model included the known resistance gene *ermB* and transposon
184 Tn6110. We were able to find *ermB* with both SEER and Kover. We also detected Tn6110-specific *k*-
185 mers with SEER while running Kover with 16-mers instead of 31-mers as in the default settings.

186 Regarding the CPU time, PhenotypeSeeker with 13-mers was faster than other tested software
187 programs (3.5 hrs vs 14-15 hrs) without losing the relevant markers in the output (Table 2). Using 16-
188 or 18-mers, the PhenotypeSeeker's running time increases but is still lower than with SEER and
189 Kover

190

191

192 **Table 2. PhenotypeSeeker comparison to Kover and SEER using *P. aeruginosa* and *C. difficile***

193 **data.** PhenotypeSeeker with the weighting option and maximum 1000 k-mers for the regression

194 model was used.

		<i>Pseudomonas aeruginosa</i> (200 genomes)			<i>Clostridium difficile</i> (460 genomes)		
		Previously known CIP resistance mutations detected			Previously known AZM resistance genes* detected		
Software	<i>k</i> -mer length	<i>gyrA</i> c.248C>T	<i>parC</i> c.260C >T	Time for model building	<i>ermB</i>	Tn6110 transposon	Time for model building
Phenotype Seeker	13	+	+	3h 36m	+	+	4h 47m
Phenotype Seeker	16	+	-	6h 51m	+	+	9h 7m
Phenotype Seeker	18	+	-	7h 31m	-	+	9h 58m
Kover	16	+	-	14h 14m	+	+	14h 10m
Kover	31	+	-	14h 46m	+	-	13h 40m
SEER	9-100	+	+	15h 7m	+	+	15h 32m

195 * As reported in Drouin *et al.* 2016 [12]

196 Discussion

197 PhenotypeSeeker works as an easy-to-use application to list the candidate biomarkers behind a studied
198 bacterial phenotype and to create a predictive model. Based on k -mers, PhenotypeSeeker does not
199 require a reference genome and is therefore also usable for species with very high intraspecific
200 variation where the selection of one genome as a reference can be complicated.

201 PhenotypeSeeker supports both discrete and continuous phenotypes as inputs. In addition, this model
202 takes into account the population structure to highlight only the possible causal variations and not the
203 mutations arising from the clonal nature of bacterial populations.

204 Unlike Kover, the PhenotypeSeeker output is not merely a trained model for predicting resistance in a
205 separate set of isolates, but the complete list of statistically significant candidate variations separating
206 antibiotic resistant and susceptible isolates for further biological interpretation is also provided.

207 Unlike SEER, PhenotypeSeeker is easier to install and can be run with only a single command for
208 building a model and another single command to use it for prediction.

209 Our tests using PhenotypeSeeker to detect antibiotic resistance markers in *P. aeruginosa* and *C.*
210 *difficile* showed that it is capable of detecting all previously known mutations in a reasonable amount
211 of time and with a relatively short k -mer length. Users can choose the k -mer length as well as decide
212 whether to use the population structure correction step. Due to the clonal nature of bacterial
213 populations, this step is highly advised for detecting genuine causal variations instead of strain-level
214 differences. In addition to a trained predictive model, the list of k -mers covering possible variations
215 related to the phenotype are produced for further interpretation by the user. The effectiveness of the
216 model can vary because of the nature of different phenotypes in different bacterial species. Simple
217 forms of antibiotic resistance that are unambiguously determined by one or two specific mutations or
218 the insertion of a gene are likely to be successfully detected by our method, and effective predictive
219 models for subsequent phenotype predictions can be created. This is supported by our prediction
220 accuracy over 96% in the *C. difficile* dataset. On the other hand, *P. aeruginosa* antibiotic resistance is
221 one of the most complicated phenotypes among clinically relevant pathogens since it is not often

222 easily described by certain single nucleotide mutations in one gene but rather through a complex
223 system involving several genes and their regulators leading to multi-resistant strains. In cases such as
224 this, the prediction is less accurate (88% in our dataset), but nevertheless, a complete list of k -mers
225 covering differentiating markers between resistant and sensitive strains can provide more insight into
226 the actual resistance mechanisms and provide candidates for further experimental testing.

227 Tests with *K. pneumoniae* virulence phenotypes showed that PhenotypeSeeker is not limited to
228 antibiotic resistance phenotypes but is potentially applicable to other measurable phenotypes as well
229 and is therefore usable in a wider range of studies.

230 Since PhenotypeSeeker input is not restricted to assembled genomes, one can skip the assembly step
231 and calculate models based on raw read data. In this case, it should be taken into account that
232 sequencing errors may randomly generate phenotype-specific k -mers; thus, we suggest using the
233 built-in option to remove low frequency k -mers. The k -mer frequency cut-off threshold depends on
234 the sequencing coverage of the genomes and is therefore implemented as user-selectable. One can
235 also build the model based on high-quality assembled genomes and then use the model for
236 corresponding phenotype prediction on raw sequencing data.

237

238 **Methods**

239 **Data**

240 PhenotypeSeeker was tested on the following three bacterial species: *Pseudomonas aeruginosa*,
241 *Clostridium difficile* and *Klebsiella pneumoniae*. The *P. aeruginosa* dataset was composed of 200
242 assembled genomes and the minimal inhibitory concentration measurements (MICs) for ciprofloxacin.
243 The *P. aeruginosa* strains were isolated during the project Transfer routes of antibiotic resistance
244 (ABRESIST) performed as part of the Estonian Health Promotion Research Programme (TerVE)
245 implemented by the Estonian Research Council, the Ministry of Agriculture (now the Ministry of
246 Rural Affairs), and the National Institute for Health Development. Isolated strains originated from
247 humans, animals and the environment (Laht et al., *Pseudomonas aeruginosa* distribution among
248 humans, animals and the environment (submitted); Telling et al., Multidrug resistant *Pseudomonas*
249 *aeruginosa* in Estonian hospitals (submitted)). Full genomes were sequenced by Illumina HiSeq2500
250 (Illumina, San Diego, USA) with paired-end, 150 bp reads (Nextera XT libraries) and de novo
251 assembled with the program SPAdes (ver 3.5.0) [32]. MICs were determined by using the epsilon meter
252 test (E-test, bioMérieux, Marcy l'Etoile, France) according to the manufacturer instructions. Binary
253 phenotypes were achieved by converting the MIC values into 0 (sensitive) and 1 (resistant)
254 phenotypes according to the European Committee on Antimicrobial Susceptibility Testing (EUCAST)
255 breakpoints [18]. The *C. difficile* dataset was composed of 460 assembled genomes received from the
256 European Nucleotide Archive [EMBL:PRJEB11776
257 (<http://www.ebi.ac.uk/ena/data/view/PRJEB11776>)] and the binary phenotypes of azithromycin
258 resistance (sensitive=0 vs resistant=1), adapted from Drouin et al., 2016 [11]. The *K. pneumoniae*
259 dataset included 167 isolates analyzed in Holt et al., 2015 [33] using human carriage status vs human
260 infection (including invasive infections) as a binary clinical phenotype (carriage=0 vs
261 invasive/infectious=1). Reads of those 167 strains were de novo assembled with SPAdes (ver 3.10.1)
262 [32]. Therefore, each test dataset was composed of pairs (x, y), where x is the bacterial genome
263 $x \in \{A,T,G,C\}^*$, and y denotes phenotype values specific to a given dataset $y \in \{0.008, \dots, 1024\}$
264 (continuous phenotype) or $y \in \{0, 1\}$ (binary phenotype).

265 **Compilation of *k*-mer lists**

266 All operations with *k*-mers are performed using the GenomeTester4 software package containing the
267 glistmaker, glistquery and glistcompare programs [14]. At first, all *k*-mers from all samples are
268 counted with glistmaker, which takes either FASTA or FASTQ files as an input and enables us to set
269 the *k*-mer length up to 32 nucleotides. Subsequently, the *k*-mers are filtered based on their frequency
270 in strains of the training set. By default, the *k*-mers that are present in or missing from less than two
271 samples are filtered out and not used in building the model. The remaining *k*-mers are used in
272 statistical testing for detection of association with the phenotype.

273 **Weighting**

274 By default, PhenotypeSeeker conducts the clonal population structure correction step by using a
275 sequence weighting approach that reduces the weight of phylogenetically closely related isolates. For
276 weighting, pairwise distances between genomes of the training set are calculated using the free
277 alignment software Mash [15]. Distances estimated by Mash are subsequently used to calculate
278 weights for each genome according to the algorithm proposed by Gerstein, Sonnhammer and Chothia
279 [16]. The calculation of GSC weights is conducted using the PyCogent python package [34]. The
280 GSC weights are taken into account while calculating Welch two-sample t-tests or chi-squared tests to
281 test the *k*-mers' associations with the phenotype. Additionally, the GSC weights can be used in the
282 final logistic regression or linear regression (if Ridge regularization is used) model generation.

283 **Chi-squared test**

284 In the case of binary phenotype input, the chi-squared test is applied to every *k*-mer that passes the
285 frequency filtration to determine the *k*-mer association with phenotype. The null hypothesis assumes
286 that there is no association between *k*-mer presence and phenotype. The alternative hypothesis
287 assumes that the *k*-mer is associated with phenotype. The chi-squared test is conducted on these
288 observed and expected values with degrees of freedom=1, using the scipy.stats Python package [35].
289 If the user selects to use the population structure correction step, then the weighted chi-squared tests
290 are conducted according to the previously published method [36].

291 **Welch two-sample t-test**

292 In the case of continuous phenotype input, the Welch two-sample t-test is applied to every k -mer that
293 passes the frequency filtration to determine if the mean phenotype values of strains having the k -mer
294 are different from the mean phenotype values of strains that do not have the k -mer. The null
295 hypothesis assumes that the strains with a k -mer have different mean phenotype values from the
296 strains without the k -mer. The alternative hypothesis assumes that the means of the strains with and
297 without the k -mer are the same. The t-test is conducted with these values using the `scipy.stats` Python
298 package [35], assuming that the samples are independent and have different variance. If the user
299 selects the population structure correction step, then the weighted t-tests are conducted [36]. In that
300 case, the p-value is calculated with the function `scipy.stats.t.sf`, which takes the absolute value of the t-
301 statistic and the value of degrees of freedom as the input.

302 **Regression analysis**

303 To perform the regression analysis, first, the x features matrix of the samples is created. The samples
304 in this matrix are strains given as the input and the features represent the k -mers that are selected for
305 the regression analysis. The values (0 or 1) in this matrix represent the presence or absence of a
306 specific k -mer in the specific strain. The target variables of this regression analysis are the resistance
307 values of the strains. Thereupon, input data are divided into training and test sets whose sizes are by
308 default 75% and 25% of the strains, respectively. In the case of a continuous phenotype, a linear
309 regression model is built, and in the case of a binary phenotype, a logistic regression model is built. In
310 both cases, the Lasso or Ridge regularization can be selected. The Lasso regularization is used by
311 default due to its ability to shrink the coefficients of non-relevant features to zero, which simplifies
312 the identification of k -mers that have the strongest association with the phenotype. To enable the
313 evaluation of the output regression model, PhenotypeSeeker provides model-evaluation metrics. For
314 the logistic regression model quality, PhenotypeSeeker provides the mean accuracy as the percentage
315 of correctly classified instances across both classes (0 and 1). Additionally, the model provides
316 averaged (and for both classes separately) precision, recall and F1-score as a weighted average of

317 precision and recall. For the linear regression model, PhenotypeSeeker provides the mean squared
318 error and the coefficient of determination of the model. To select for the best regularization parameter
319 alpha, a k-fold cross-validation on the training data is performed. By default, 25 alpha values spaced
320 evenly on a log scale from 1E-6 to 1E6 are tested with 10-fold cross-validation and the model with the
321 best mean accuracy (logistic regression) or with the best coefficient of determination (linear
322 regression) is saved to the output file. Regression analysis is conducted using the sklearn.linear_model
323 Python package [37].

324 **Parameters used for training and testing**

325 Our models were created using mainly k-mer length 13 (“-l 13”; default). We counted the k-mers that
326 occurred at least once per sample (“-c 1”; default) when the analysis was performed on contigs or at
327 least five times per sample (“-c 5”) when the analysis was performed on raw reads. In the first
328 filtering step, we filtered out the k-mers that were present in or missing from less than two samples (“-
329 -min 2 --max 2”; default) when the analysis was performed on a binary phenotype or fewer than ten
330 samples (“--min 10 --max N-10”; N – total number of samples) when the analysis was performed on a
331 continuous phenotype. In the next filtering step, we filtered out the k-mers with a statistical test p-
332 value larger than 0.05 (“-p_value 0.05”; default).

333 The regression analysis was performed with a maximum of 1000 lowest p-valued k-mers (“-n_kmers;
334 1000”; default) when the analysis was done with binary phenotype and with a maximum of 10,000
335 lowest p-valued k-mers (“-n_kmers 10000”; default) when the analysis was performed with a
336 continuous phenotype. For regression analyses, we split our datasets into training (75%)
337 and test (25%) sets (“-s 0.25”; default). The regression analyses were conducted using Lasso
338 regularization (“-r L1”; default), and the best regularization parameter was picked from the 25
339 regularization parameters spaced evenly on a log scale from 1E-6 to 1E6 (“-n_alphas 25 --alpha_min
340 1E-6 --alpha_max 1E6”; default). The model performances with each regularization parameter were
341 evaluated by cross-validation with 10-folds (“-n_splits 10”; default).

342 The correction for clonal population structure (“--weights +”; default) and assembly of k-mers used in
343 the regression model (“--assembly +”; default) were conducted in all our analyses.

344 **Comparison to existing software**

345 SEER was installed and run on a local server with 32 CPU cores and 512 GB RAM, except the final
346 step, which we were not able to finish without segmentation fault. This last SEER step was launched
347 via VirtualBox in <ftp://ftp.sanger.ac.uk/pub/pathogens/pathogens-vm/pathogens-vm.latest.ova>. Both
348 binary and continuous phenotypes were tested for *P. aeruginosa* and the binary phenotype in *C.*
349 *difficile* cases. Default settings were used. Kover was installed on a local server and used with the
350 settings suggested by the authors in the program tutorial.

351 **Acknowledgements**

352 The authors are grateful to Triinu Kõressaar for her invaluable suggestions toward improvement of
353 the manuscript.

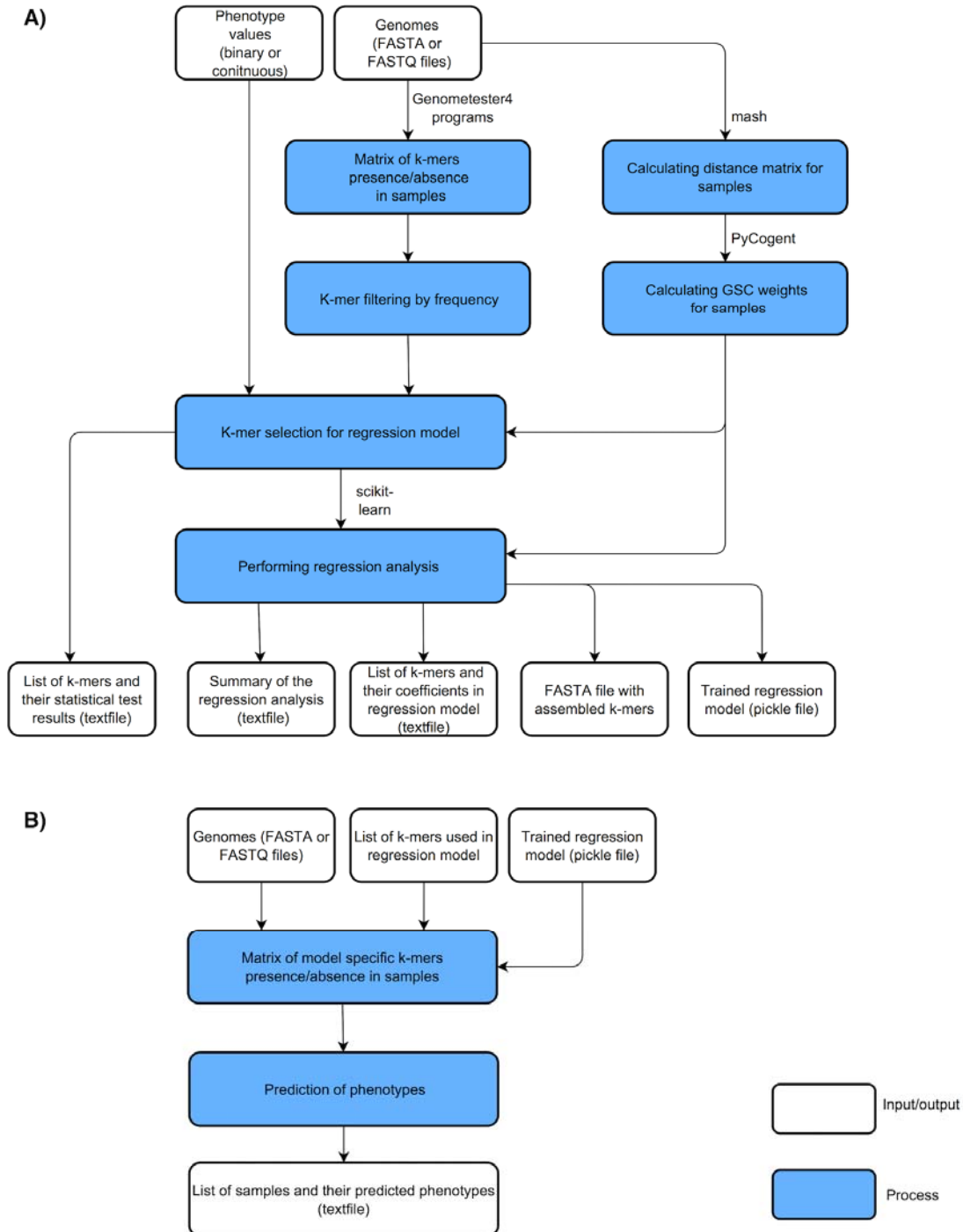
354 **Supporting information**

355 **S1 File. The effects of different p-value cut-offs on model performances.** (PDF)

356 **S2 File. Phylogenetic trees and isolate specific information of the studied *P. aeruginosa*, *C.*
357 *difficile* and *K. pneumoniae* isolates.** (XLSX)

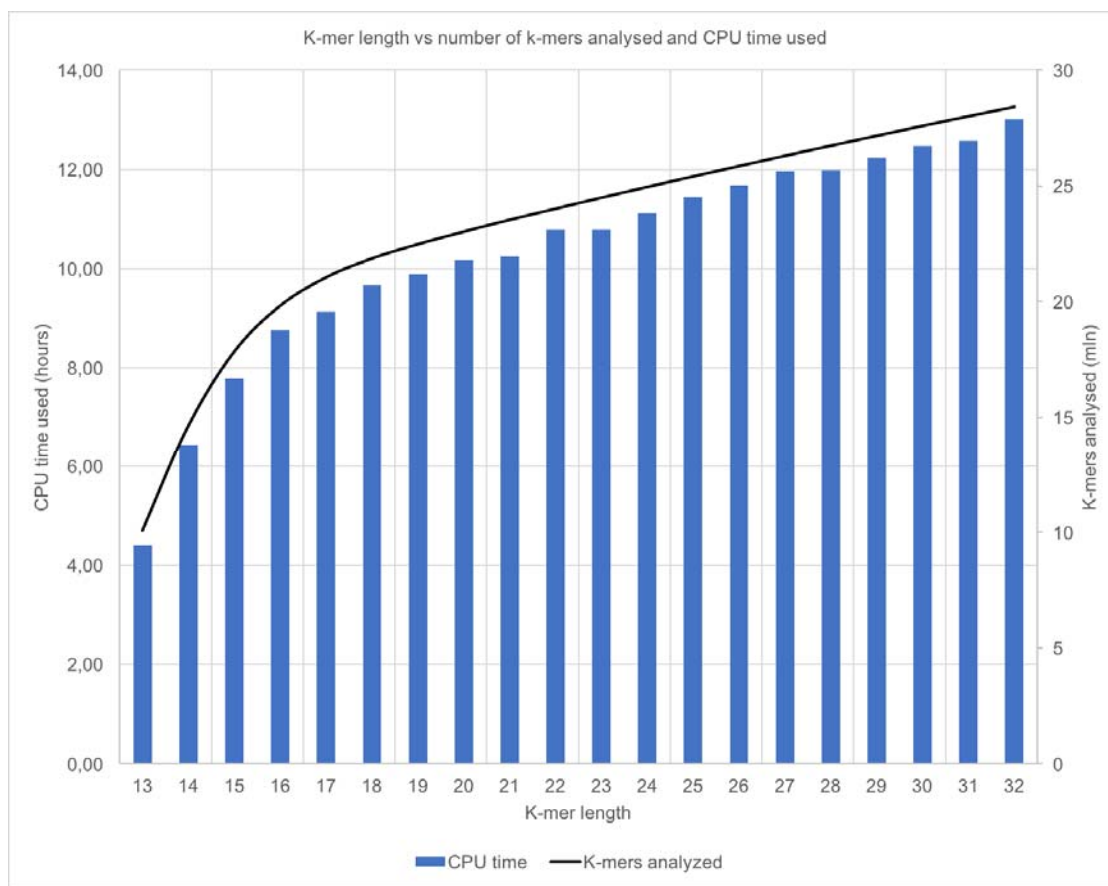
358

359 **Figures**



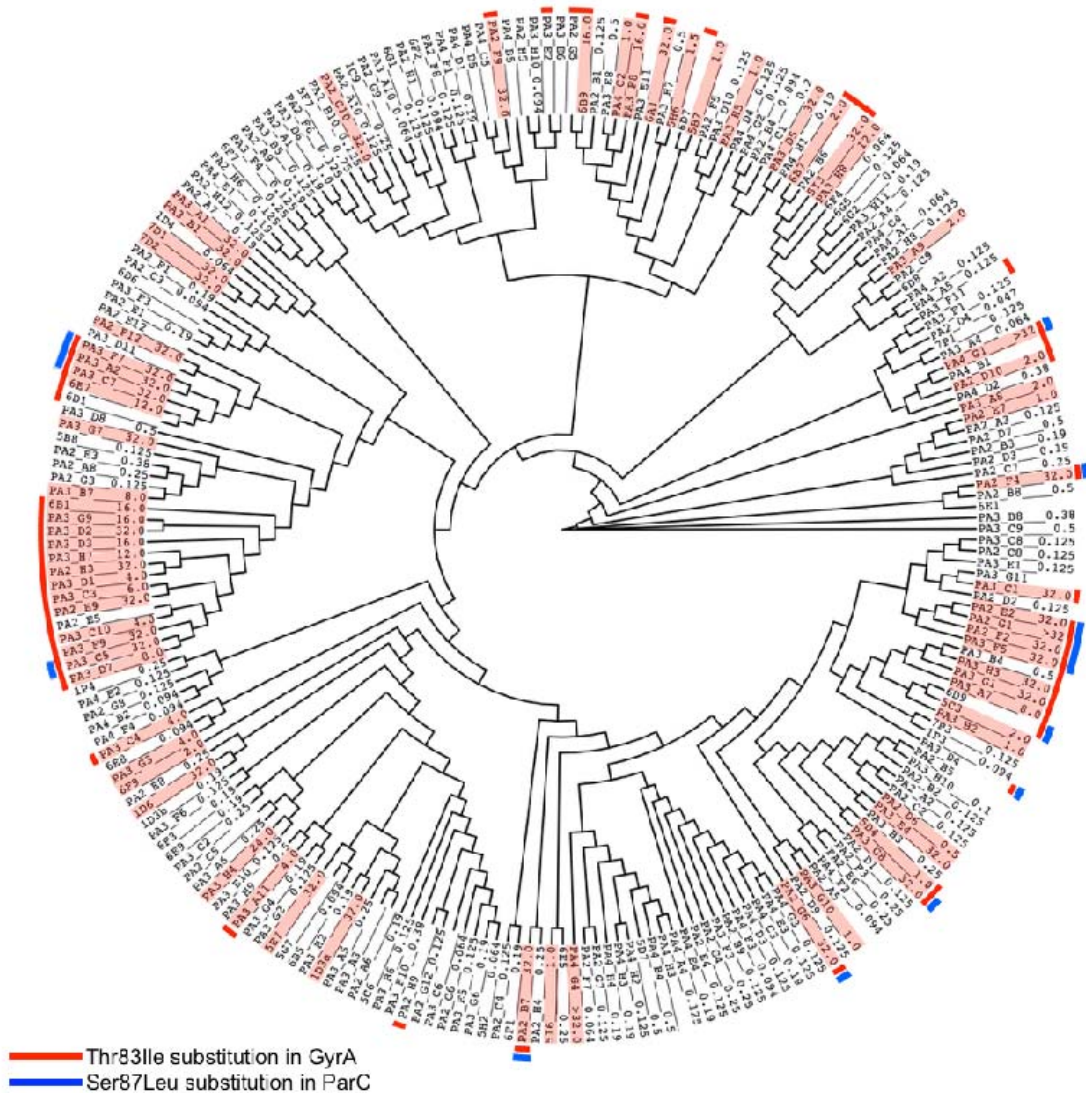
360

361 **Fig 1. Schematic presentation of PhenotypeSeeker workflow.** Panel A shows the 'PhenotypeSeeker
362 modeling' steps, which generate the phenotype prediction model based on the input genomes and their
363 phenotype values. Panel B shows the 'PhenotypeSeeker prediction' steps, which use the previously
364 generated model to predict the phenotypes for input genomes.



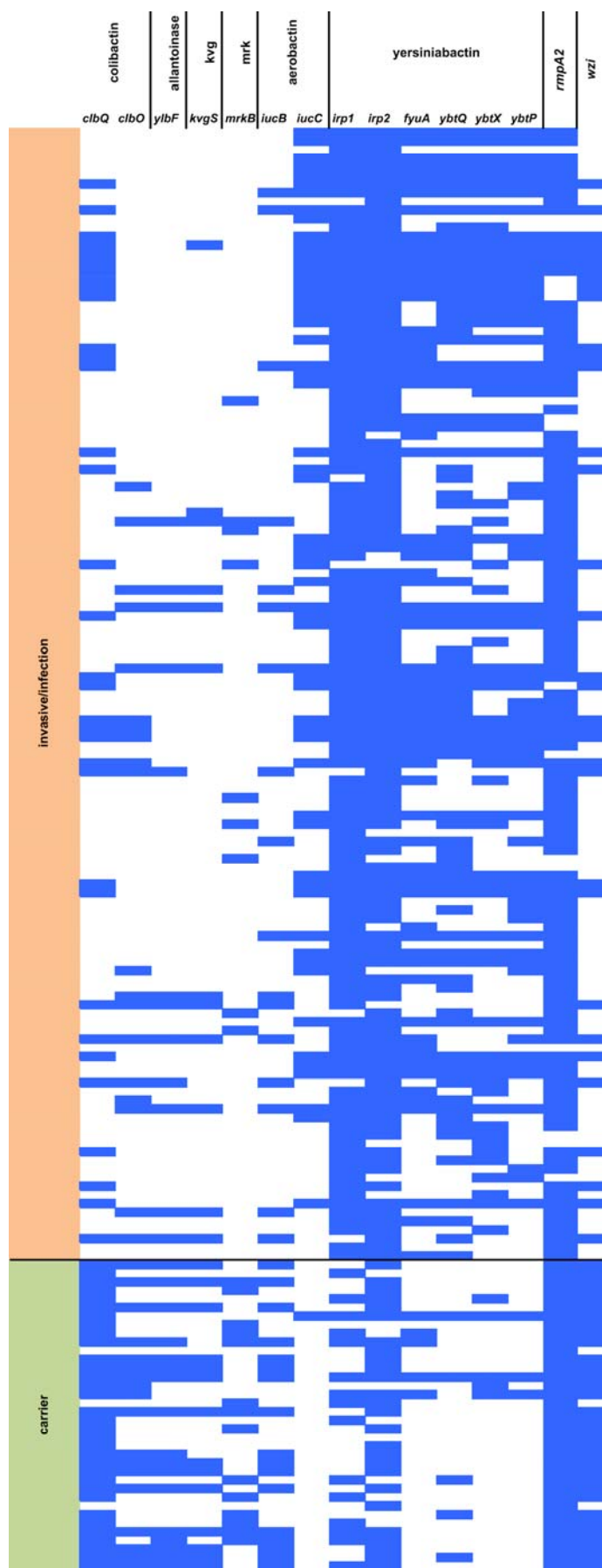
365

366 **Fig 2. The influence of k -mer length on the CPU time of PhenotypeSeeker (bars, left axis) and**
367 **on the number of different k -mers present in the genomes (line, right axis).**

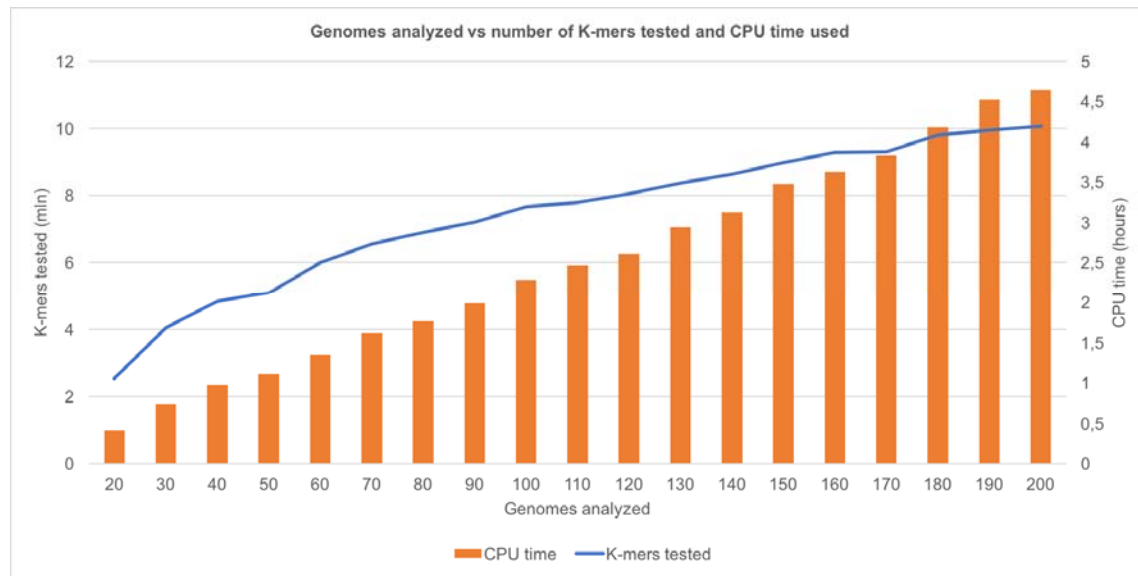


368

369 **Fig 3. The positions of ciprofloxacin-resistant *P. aeruginosa* strains on cladogram.** The MIC
370 values (mg/l) are marked to the external nodes with corresponding strain names. Strains with MIC >
371 0.5 mg/l are highlighted with pink to denote ciprofloxacin resistance according to EUCAST
372 breakpoints [18]. Strains with detected mutations in QRDR of *gyrA* and *parC* are marked with the
373 color code on the perimeter of the cladogram.



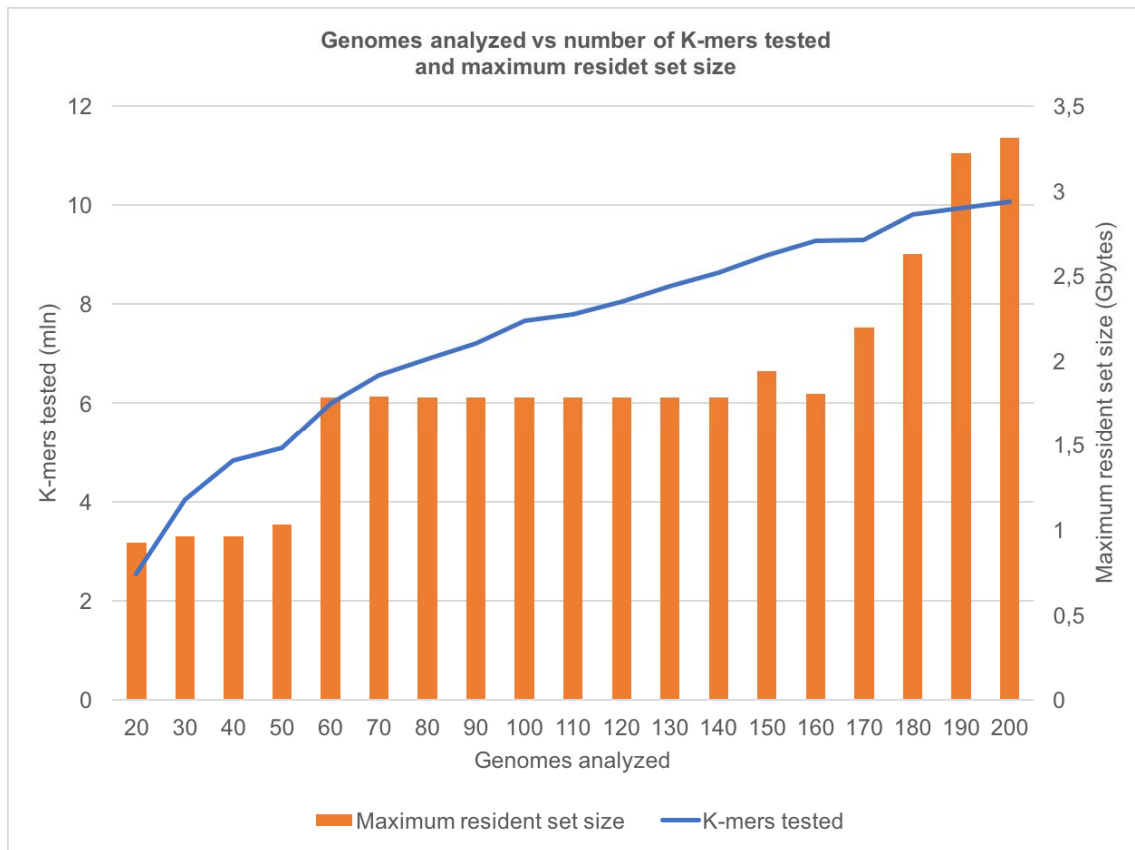
375 **Fig 4. Virulence genes in corresponding clusters and *wzi* included in the PhenotypeSeeker**
376 **prediction model in *K. pneumoniae* strains (13-mers, weighted, max. 10 000 *k*-mers for the**
377 **regression model).** Each row is one strain, and each column represents one protein coding gene. Blue
378 cells represent 13-mers in the model for the corresponding gene and a strain. Genes in colibactin,
379 aerobactin and yersiniabactin clusters show the most differentiating pattern between carrier and
380 invasive/infectious strains. Virulence genes belonging to the same clusters but without 13-mers in the
381 prediction model are not shown.



382

383 **S1 Fig. Relationship between the number of input genomes and the CPU time.** The

384 PhenotypeSeeker CPU time depends mainly on the number of different k-mers in input genomes and
385 on computations made with every genome. The analysis performed on our 200 *P. aeruginosa* genomes
386 showed that the PhenotypeSeeker CPU time has a good linear relationship ($R^2=0.997$) with the
387 number of genomes given as input. Although the number of k-mers grows logarithmically with the
388 number of genomes given as input, the linear relationship is because some of the computations made
389 with every genome are more time-consuming when there are larger numbers of different k-mers
390 present in the input genomes.



391

392 **S2 Fig. Relationship between the number of input genomes and RAM memory usage.** The
393 maximum resident set size of PhenotypeSeeker increases in steps with the number of genomes that are
394 given as the input for model training. This is due to the fact that the maximum resident set size of
395 PhenotypeSeeker is defined by the size of the Python dictionary object into which all different k-mers
396 and their frequencies in genomes are stored. The Python dictionary uses a hash table implementation,
397 and the size of the hash table doubles when it is two thirds full. Therefore, when more genomes are
398 analyzed, more different k-mers are stored into the hash table, and if a certain threshold is exceeded,
399 the next step in the maximum resident set size is taken. However, if the regression is performed with a
400 large number of k-mers, the regression could easily become the most memory using part of the
401 analysis as the data matrix (k-mers x samples), read into memory, grows larger (analysis with 150,
402 170, 180, 190 and 200 genomes).

403 References

- 404 1. Kisand V, Lettieri T. Genome sequencing of bacteria: sequencing, de novo assembly and
405 rapid analysis using open source tools. *BMC Genomics* [Internet]. 2013;14(1):1. Available
406 from: *BMC Genomics*
- 407 2. Bertelli C, Greub G. Rapid bacterial genome sequencing: Methods and applications in clinical
408 microbiology. *Clin Microbiol Infect* [Internet]. 2013;19(9):803–13. Available from:
409 <http://dx.doi.org/10.1111/1469-0691.12217>
- 410 3. Didelot X, Bowden R, Wilson DJ, Peto TEA, Crook DW. Transforming clinical microbiology
411 with bacterial genome sequencing. *Nat Rev Genet*. 2012;13(9):601–12.
- 412 4. Laabei M, Recker M, Rudkin JK, Aldeljawi M, Gulay Z, Sloan TJ, et al. Predicting the
413 virulence of MRSA from its genome sequence. *Genome Res*. 2014;24(5):839–49.
- 414 5. Weinert LA, Chaudhuri RR, Wang J, Peters SE, Corander J, Jombart T, et al. Genomic
415 signatures of human and animal disease in the zoonotic pathogen *Streptococcus suis*. *Nat*
416 *Commun*. 2015;6.
- 417 6. Chen PE, Shapiro BJ. The advent of genome-wide association studies for bacteria. *Curr Opin*
418 *Microbiol* [Internet]. 2015;25:17–24. Available from:
419 <http://dx.doi.org/10.1016/j.mib.2015.03.002>
- 420 7. Köser CU, Ellington MJ, Peacock SJ. Whole-genome sequencing to control antimicrobial
421 resistance. *Trends Genet*. 2014;30(9):401–7.
- 422 8. WHO. Antimicrobial resistance. Global Report on Surveillance. *Bull World Health Organ*
423 [Internet]. 2014;61(3):383–94. Available from:
424 <http://www.ncbi.nlm.nih.gov/pubmed/22247201%5Cnhttp://www.pubmedcentral.nih.gov/articlerender.fcgi?artid=2536104&tool=pmcentrez&rendertype=abstract>
- 426 9. Crofts TS, Gasparrini AJ, Dantas G. Next-generation approaches to understand and combat the
427 antibiotic resistance. *Nat Rev Microbiol* [Internet]. 2017;15(7):422–34. Available from:
428 <http://dx.doi.org/10.1038/nrmicro.2017.28>
- 429 10. Bakour S, Sankar SA, Rathored J, Biagini P, Raoult D, Fournier P-E. Identification of
430 virulence factors and antibiotic resistance markers using bacterial genomics. *Future Microbiol*
431 [Internet]. 2016;11(3):455–66. Available from:
432 <http://www.futuremedicine.com/doi/10.2217/fmb.15.149>
- 433 11. Lees JA, Vehkala M, Välimäki N, Harris SR, Chewapreecha C, Croucher NJ, et al. Sequence
434 element enrichment analysis to determine the genetic basis of bacterial phenotypes. *Nat*
435 *Commun* [Internet]. 2016;7:12797. Available from:
436 <http://www.nature.com/doi/10.1038/ncomms12797>
- 437 12. Drouin A, Giguère S, Déraspe M, Marchand M, Tyers M, Loo VG, et al. Predictive
438 computational phenotyping and biomarker discovery using reference-free genome
439 comparisons. *BMC Genomics* [Internet]. 2016;17(1):754. Available from:
440 <http://bmcgenomics.biomedcentral.com/articles/10.1186/s12864-016-2889-6>
- 441 13. Marinier E, Zaheer R, Berry C, Weedmark KA, Domaratzki M, Mabon P, et al. Neptune: a
442 bioinformatics tool for rapid discovery of genomic variation in bacterial populations. *Nucleic*
443 *Acids Res* [Internet]. 2017; Available from:
444 [http://academic.oup.com/nar/article/doi/10.1093/nar/gkx702/4083563/Neptune-a-](http://academic.oup.com/nar/article/doi/10.1093/nar/gkx702/4083563/Neptune-a-bioinformatics-tool-for-rapid-discovery)
445 [bioinformatics-tool-for-rapid-discovery](http://academic.oup.com/nar/article/doi/10.1093/nar/gkx702/4083563/Neptune-a-bioinformatics-tool-for-rapid-discovery)
- 446 14. Kaplinski L, Lepamets M, Remm M. GenomeTester4: a toolkit for performing basic set
447 operations - union, intersection and complement on k-mer lists. *Gigascience* [Internet].

- 448 2015;4(1):58. Available from: <https://academic.oup.com/gigascience/article-lookup/doi/10.1186/s13742-015-0097-y>
449
- 450 15. Ondov BD, Treangen TJ, Melsted P, Mallonee AB, Bergman NH, Koren S, et al. Mash: fast
451 genome and metagenome distance estimation using MinHash. *Genome Biol* [Internet].
452 2016;17(1):132. Available from:
453 <http://genomebiology.biomedcentral.com/articles/10.1186/s13059-016-0997-x>
- 454 16. Gerstein M, Sonnhammer EL, Chothia C. Volume changes in protein evolution. *J Mol Biol*.
455 1994;236(4):1067–78.
- 456 17. Pajuste F-D, Kaplinski L, Möls M, Puurand T, Lepamets M, Remm M. FastGT: an alignment-
457 free method for calling common SNVs directly from raw sequencing reads. *Sci Rep* [Internet].
458 2017;7(1):2537. Available from: <http://www.nature.com/articles/s41598-017-02487-5>
- 459 18. SusceptibilityTesting EC on A. European Committee on Antimicrobial Susceptibility Testing
460 Breakpoint tables for interpretation of MICs and zone diameters European Committee on
461 Antimicrobial Susceptibility Testing Breakpoint tables for interpretation of MICs and zone
462 diameters.
463 http://www.eucast.org/fileadmin/src/media/PDFs/EUCAST_files/Breakpoint_tables/v_50_Breakpoint_Table_01.pdf [Internet]. 2015;0–77. Available from:
464 http://www.eucast.org/fileadmin/src/media/PDFs/EUCAST_files/Breakpoint_tables/v_5.0_Breakpoint_Table_01.pdf
465
466
- 467 19. Fàbrega A, Madurga S, Giralt E, Vila J. Mechanism of action of and resistance to quinolones.
468 *Microb Biotechnol*. 2009;2(1):40–61.
- 469 20. Jalal S, Wretling B. Mechanisms of quinolone resistance in clinical strains of *Pseudomonas*
470 *aeruginosa*. *Microb Drug Resist* [Internet]. 1998;4(4):257–61. Available from:
471 <http://www.ncbi.nlm.nih.gov/pubmed/9988043>
- 472 21. Kaminska KH, Purta E, Hansen LH, Bujnicki JM, Vester B, Long KS. Insights into the
473 structure, function evolution of the radical-SAM 23S rRNA methyltransferase Cfr that confers
474 antibiotic resistance in bacteria. *Nucleic Acids Res*. 2009;38(5):1652–63.
- 475 22. Carniel E. The *Yersinia* high-pathogenicity island: An iron-uptake island. *Microbes Infect*.
476 2001;3(7):561–9.
- 477 23. Chen YT, Chang HY, Lai YC, Pan CC, Tsai SF, Peng HL. Sequencing and analysis of the
478 large virulence plasmid pLVPK of *Klebsiella pneumoniae* CG43. *Gene*. 2004;337(1–2):189–
479 98.
- 480 24. Lagos R, Baeza M, Corsini G, Hetz C, Strahsburger E, Castillo JA, et al. Structure,
481 organization and characterization of the gene cluster involved in the production of microcin
482 E492, a channel-forming bacteriocin. *Mol Microbiol*. 2001;42(1):229–43.
- 483 25. Nassif X, Sansonetti PJ. Correlation of the virulence of *Klebsiella pneumoniae* K1 and K2
484 with the presence of a plasmid encoding aerobactin. *Infect Immun*. 1986;54(3):603–8.
- 485 26. Putze J, Hennequin C, Nougayrède JP, Zhang W, Homburg S, Karch H, et al. Genetic structure
486 and distribution of the colibactin genomic island among members of the family
487 *Enterobacteriaceae*. *Infect Immun*. 2009;77(11):4696–703.
- 488 27. Chou HC, Lee CZ, Ma LC, Fang CT, Chang SC, Wang JT. Isolation of a chromosomal region
489 of *Klebsiella pneumoniae* associated with allantoin metabolism and liver infection. *Infect*
490 *Immun*. 2004;72(7):3783–92.
- 491 28. Cheng HY, Chen YS, Wu CY, Chang HY, Lai YC, Peng HL. RmpA regulation of capsular
492 polysaccharide biosynthesis in *Klebsiella pneumoniae* CG43. *J Bacteriol*. 2010;192(12):3144–
493 58.

- 494 29. Lai Y, Peng H, Chang H. RmpA2, an Activator of Capsule Biosynthesis in. MBio.
495 2003;185(3):788–800.
- 496 30. Ma L-C, Fang C-T, Lee C-Z, Shun C-T, Wang J-T. Genomic heterogeneity in *Klebsiella*
497 *pneumoniae* strains is associated with primary pyogenic liver abscess and metastatic infection.
498 J Infect Dis [Internet]. 2005;192(1):117–28. Available from:
499 <http://www.ncbi.nlm.nih.gov/pubmed/15942901>
- 500 31. Lai Y-C, Lin G-T, Yang S-L, Chang H-Y, Peng H-L, S. I, et al. Identification and
501 characterization of KvgAS, a two-component system in *Klebsiella pneumoniae* CG43. FEMS
502 Microbiol Lett [Internet]. 2003;218(1):121–6. Available from:
503 <https://academic.oup.com/femsle/article-lookup/doi/10.1111/j.1574-6968.2003.tb11507.x>
- 504 32. Bankevich A, Nurk S, Antipov D, Gurevich AA, Dvorkin M, Kulikov AS, et al. SPAdes: A
505 New Genome Assembly Algorithm and Its Applications to Single-Cell Sequencing. J Comput
506 Biol [Internet]. 2012;19(5):455–77. Available from:
507 <http://online.liebertpub.com/doi/abs/10.1089/cmb.2012.0021>
- 508 33. Holt KE, Wertheim H, Zadoks RN, Baker S, Whitehouse CA, Dance D, et al. Genomic
509 analysis of diversity, population structure, virulence, and antimicrobial resistance in *Klebsiella*
510 *pneumoniae*, an urgent threat to public health. Proc Natl Acad Sci [Internet].
511 2015;112(27):E3574–81. Available from:
512 <http://www.pnas.org/lookup/doi/10.1073/pnas.1501049112>
- 513 34. Knight R, Maxwell P, Birmingham A, Carnes J, Caporaso JG, Easton BC, et al. PyCogent: a
514 toolkit for making sense from sequence. Genome Biol [Internet]. 2007;8(8):R171. Available
515 from: <http://genomebiology.biomedcentral.com/articles/10.1186/gb-2007-8-8-r171>
- 516 35. SciPy Community. SciPy Reference Guide 0.16.0. 2013;1229.
- 517 36. Josh Pasek A, Gene Culter by, Schwemmler Maintainer Josh Pasek M. Package “weights”
518 with some assistance from Alex Tahk and some code modified from R- core; Additional
519 contributions. 2016; Available from: [https://cran.r-](https://cran.r-project.org/web/packages/weights/weights.pdf)
520 [project.org/web/packages/weights/weights.pdf](https://cran.r-project.org/web/packages/weights/weights.pdf)
- 521 37. Pedregosa F, Varoquaux G, Gramfort A, Michel V, Thirion B, Grisel O, et al. Scikit-learn:
522 Machine Learning in Python. J Mach Learn Res [Internet]. 2011;12:2825–2830. Available
523 from:
524 http://dl.acm.org/citation.cfm?id=1953048.2078195%5Cnhttp://dl.acm.org/ft_gateway.cfm?id
525 [=2078195&type=pdf](http://dl.acm.org/ft_gateway.cfm?id=2078195&type=pdf)
- 526